



DOI: 10.22144/ctu.jen.2018.051

## Plasmon excitation in MLG-GaAs heterostructure - Analytical expressions in long-wavelength limit

Nguyen Van Men\* and Dong Thi Kim Phuong

Department of Physics, Faculty of Education, An Giang University, Vietnam

\*Correspondence: Nguyen Van Men (email: nvmen@agu.edu.vn)

### Article info.

Received 29 Jan 2018  
Revised 11 May 2018  
Accepted 30 Nov 2018

### Keywords

Dielectric function, plasmon excitation, random-phase-approximation

### ABSTRACT

Plasmon excitation plays important roles in many-body systems' properties such as screening and drag in layer structures and is applied in plasmonic and photonic technology. This research is to consider the analytical expressions of plasmon frequencies in a double layer system made of mono-layer graphene and GaAs quantum well with separation of  $d$  and nonhomogeneous dielectric background at zero temperature. In this research, random-phase-approximation is used to calculate the dielectric function of the system and to determine the plasmon modes by finding out zeroes of the function. Results present that the zeroes of dielectric function admit two solutions (as in the case of semiconductor double quantum well systems or double-layer graphene), corresponding to optical and acoustic branch, respectively. Meanwhile, the frequency of the former is proportional to root square of wave vector and depends on the dielectric constant of the surrounding layers; the frequency of the later is proportional to wave vector and depends on dielectric constant of contacting media and quantum well in long wavelength limit.

Cited as: Men, N.V. and Phuong, D.T.K., 2018. Plasmon excitation in MLG-GaAs heterostructure - Analytical expressions in long-wavelength limit. Can Tho University Journal of Science. 54(8): 154-159.

## 1 INTRODUCTION

It is the fact that both of the unique electronic properties (Neto *et al.*, 2009; Sarma *et al.*, 2010) and possible technological application (Geim and Novoselov, 2007) of graphene attract a lot of attention from many theoretical and experimental researchers in recent years. One of important different characteristics of mono-layer graphene (MLG) is that quasi-particle excitations in this material have a linear dispersion at low energies and are described by the massless Dirac equation (Sarma *et al.*, 2010). Because of this different property, the plasmon of double layer systems consisting of MLG would be predicted to have lots of significant differences from those of single layer one.

Plasmon excitations in many-electron systems, an important property, have been studied for a long time and have been used to create plasmonic and photonic devices (Maier, 2007). The dynamical dielectric function and plasmon dispersion relation are two important many-body quantities in such structures (Vazifeshenas *et al.*, 2010). Therefore, it can be seen that the dielectric function and plasmon mode of two-dimensional electron gas (2DEG) were calculated both with and without correlation (Khanh, 1996 and 2001; Khanh and Toan, 2003). Besides, dielectric function and plasmon dispersion of MLG and bi-layer graphene (BLG) were considered by Hwang and Sarma (2007) and by Sensarma *et al.* (2010). On the other hand, double-layer structures have been studied in

recent years such as double-layer graphene (DLG) with homogeneous dielectric background at both zero and finite temperature (Hwang and Sarma, 2009; Tuan and Khanh, 2013) with numerical and analytical in long wavelength limit, DLG with nonhomogeneous dielectric background at finite temperature (Badalyan and Peeters, 2012), plasmon modes of double-layer structures consisting of MLG and very thin 2DEG sheet at zero temperature (Principi *et al.*, 2012). In that work, Principi *et al.* (2012) have shown that long-range Coulomb interactions between massive electrons and massless Dirac fermions lead to a new set of optical and acoustic intra-subband plasmons. An analytical result for plasmon frequency has been found for this kind of system. Similarly, another analytical result for plasmon frequencies in a BLG – 2DEG system has been shown by Nguyen Van Men and Nguyen Quoc Khanh (2017). Finally, recent researches relevant to graphene studied in India (Digish, 2015) and in Vietnam (Ho Sy Ta, 2017) showed the interest of material scientists in graphene. It is the fact that although collective excitations of such chiral-nonchiral double-layer structures (MLG – 2DEG as an example) may have interesting properties, this property of MLG-2DEG systems including layer-thickness of 2DEG sheet and nonhomogeneous background has not been paid enough attention by physicists.

Because of above reasons, this paper considers a double-layer system consisting of doped MLG and GaAs quantum well, separated by a spacer of width  $d$  assuming that 2DEGs in MLG and GaAs are electrically isolated (Gamucci *et al.*, 2014). Inhomogeneity of the background and 2DEG layer-thickness are taken into account in calculations. An analytical expression for plasmon frequencies would be final destination.

**2 THEORY**

The consideration double-layer system is made of a MLG flake placed onto modulation-doped GaAs/AlGaAs heterostructure hosting a 2DEG, with the effective electron mass  $m^*$  in the GaAs quantum well as shown in Fig. 1.

$$\begin{aligned} \varepsilon_{2\text{DEG-g}}(q,\omega) = & 1 + U_{2\text{DEG}}(q)\Pi_{2\text{DEG}}(q,\omega) + U_g(q)\Pi_g(q,\omega) + \\ & \left\{ U_{2\text{DEG}}(q)U_g(q) - [U_{g-2\text{DEG}}(q)]^2 \right\} \Pi_{2\text{DEG}}(q,\omega)\Pi_g(q,\omega) \end{aligned} \tag{4}$$

where  $\Pi_{2\text{DEG}}(q,\omega)$  and  $\Pi_g(q,\omega)$  are the zero-temperature non-interacting density-density response functions of the 2DEG and MLG, respectively (Stern, 1967; Czachora *et al.*, 1982; Sarma

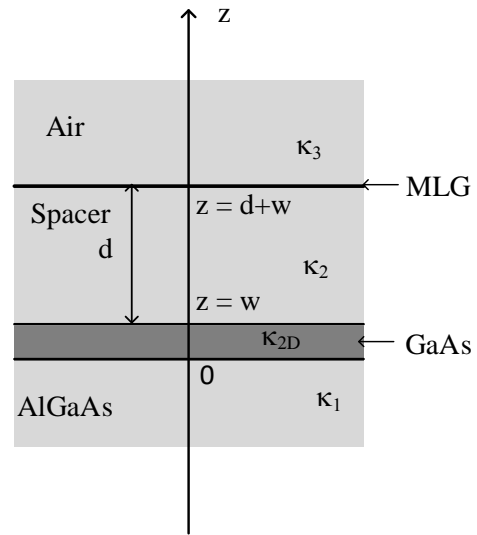


**Fig. 1: A MLG-2DEG double-layer system immersed in a three-layered different dielectric medium  $\kappa_1, \kappa_2,$  and  $\kappa_3$**

The plasmon dispersion relation of an electronic system can be obtained from the zeroes of dynamical dielectric function (Sarma and Madhukar, 1981; Hwang and Sarma, 2009).

$$\varepsilon(q,\omega_p - i\gamma) = 0 \tag{1}$$

Where  $\omega_p$  is the plasmon frequency at a given wave-vector  $q$  and  $\gamma$  is the damping rate of plasma oscillations. In case of weak damping ( $\gamma \ll \omega_p$ ), the plasmon dispersion and decay rate are determined from the following equations (Tanatar and Davoudi, 2003; Vazifeshenas *et al.*, 2010).

$$\text{Re} \varepsilon(q,\omega_p) = 0 \tag{2}$$

$$\gamma = \text{Im} \varepsilon(q,\omega_p) \left( \left. \frac{\partial \text{Re} \varepsilon(q,\omega)}{\partial \omega} \right|_{\omega=\omega_p} \right)^{-1} \tag{3}$$

In the random-phase-approximation (RPA), the dynamical dielectric function of MLG-2DEG double-layer system has the form (Vazifeshenas *et al.*, 2010; Tuan and Khanh, 2013; Badalyan and Peeters, 2012).

*et al.*, 2010 and 2011).  $U_{2\text{DEG/g}}(q)$  and  $U_{g-2\text{DEG}}(q)$  are the intra- and inter-layer bare Coulomb interactions in momentum space found out by solving

Poisson equation (Scharf and Matos-Abiague, 2012).

$$U_{g-2DEG}(q) = \frac{8\pi e^2}{q} f_{g-2DEG}(qd, qw) \tag{6}$$

$$U_{2DEG/g}(q) = \frac{4\pi e^2}{q} f_{2DEG/g}(qd, qw) \tag{5} \quad \text{Where}$$

$$f_{g-2DEG}(x, y) = \frac{2\pi^2 \kappa_2 \{ \kappa_1 [\cosh(y) - 1] + \kappa_{2D} \sinh(y) \}}{y(y^2 + 4\pi^2) N(x, y)} \tag{7}$$

$$f_g(x, y) = \frac{\kappa_2 \cosh(x) [\kappa_1 \sinh(y) + \kappa_{2D} \cosh(y)] + \kappa_{2D} \sinh(x) [\kappa_1 \cosh(y) + \kappa_{2D} \sinh(y)]}{N(x, y)} \tag{8}$$

$$f_{2DEG}(x, y) = \frac{\kappa_1 \kappa_2 [\kappa_2 \sinh(x) + \kappa_3 \cosh(x)] \{ 64\pi^4 [1 - \cosh(y)] + y(y^2 + 4\pi^2) (3y^2 + 8\pi^2) \sinh(y) \}}{2\kappa_{2D} y^2 (y^2 + 4\pi^2)^2 N(x, y)} + \frac{[\kappa_2 (\kappa_1 + \kappa_3) \cosh x + (\kappa_2^2 + \kappa_1 \kappa_3) \sinh x] [y(32\pi^4 + 20\pi^2 y^2 + 3y^4) \cosh y - 32\pi^4 \sinh y]}{2y^2 (y^2 + 4\pi^2)^2 N(x, y)} + \frac{\kappa_{2D} [\kappa_2 \cosh x + \kappa_3 \sinh x] y (y^2 + 4\pi^2) (3y^2 + 8\pi^2) \sinh y}{2y^2 (y^2 + 4\pi^2)^2 N(x, y)} \tag{9}$$

$$N(x, y) = \kappa_2 \cosh x [\kappa_{2D} (\kappa_1 + \kappa_3) \cosh y + (\kappa_1 \kappa_3 + \kappa_{2D}^2) \sinh y] + \sinh x [\kappa_{2D} (\kappa_2^2 + \kappa_1 \kappa_3) \cosh y + (\kappa_1 \kappa_2^2 + \kappa_3 \kappa_{2D}^2) \sinh y] \tag{10}$$

It can be seen that the dielectric function of MLG-2DEG is evidently complicated. Hence, the analytical solution of Eq. (2) can be found only in approximation.

### 3 RESULTS AND DISCUSSION

This section illustrates the analytical solutions of

$$\omega_{\pm}^2 = \frac{q}{2} \left\{ \omega_{02DEG}^2 f_{2DEG}(qd, qw) + \omega_{0g}^2 f_g(qd, qw) \pm \text{Sqrt} \left[ \left[ \omega_{02DEG}^2 f_{2DEG}(qd, qw) \right]^2 + \left[ \omega_{0g}^2 f_g(qd, qw) \right]^2 + 2\omega_{02DEG}^2 \omega_{0g}^2 \left[ 2[f_{g-2DEG}(qd, qw)]^2 - f_{2DEG}(qd, qw) f_g(qd, qw) \right] \right] \right\} \tag{11}$$

where  $\omega_{02DEG}^2 = \frac{2\pi e^2 n_{2DEG}}{m^*}$  and  $\omega_{0g}^2 = \frac{2e^2 v_F \sqrt{\pi n_g}}{\hbar}$ , and  $v_F$  is graphene velocity. Here  $n_{2DEG}$  and  $n_g$  are the density of carriers in 2DEG and MLG, respectively. In limit  $q \rightarrow 0$ , we have  $qd \ll 1$

Eq. (2) with long wavelength approximation calculations. Using long wavelength expansions of  $\Pi_{2DEG}(q, \omega)$  and  $\Pi_g(q, \omega)$  (Czachora *et al.*, 1982; Sarma *et al.*, 2011), Eq. (2) admits the following solutions:

and  $qw \ll 1$ , hence  $f_{2DEG}(qd, qw)$ ,  $f_g(qd, qw)$ , and  $f_{g-2DEG}(qd, qw)$  shown in Eqs. (7), (8), (9) can be expanded to the first order of  $q$ , and get

$$f_{2DEG}(qd, qw) = \frac{2}{\kappa_1 + \kappa_3} + \left[ \frac{2(\kappa_3^2 - \kappa_2^2)}{\kappa_2(\kappa_1 + \kappa_3)^2} d + \left[ \frac{5}{4\kappa_{2D}\pi^2} + \frac{2(\kappa_1^2 - 3\kappa_{2D}^2 - \kappa_1\kappa_3 + \kappa_3^2)}{3\kappa_{2D}(\kappa_1 + \kappa_3)^2} \right] w \right] q \tag{12}$$

$$f_{g-2DEG}(qd, qw) = \frac{2}{\kappa_1 + \kappa_3} + \left[ \frac{2(\kappa_2^2 + \kappa_1 \kappa_3)}{\kappa_2(\kappa_1 + \kappa_3)^2} d + \frac{(\kappa_1^2 \kappa_2 - 2\kappa_2 \kappa_2^2 D - \kappa_1 \kappa_2 \kappa_3)}{\kappa_2 \kappa_2 D (\kappa_1 + \kappa_3)^2} w \right] q \quad (13)$$

$$f_g(qd, qw) = \frac{2}{\kappa_1 + \kappa_3} + \left[ \frac{2(\kappa_1^2 - \kappa_2^2)}{\kappa_2(\kappa_1 + \kappa_3)^2} d + \frac{2(\kappa_1^2 - \kappa_2^2 D)}{\kappa_2 D (\kappa_1 + \kappa_3)^2} w \right] q \quad (14)$$

Replace Eqs. (12), (13), and (14) into Eq. (11). Note that in the case of plus sign, only the first order of  $q$  is kept, Eq. (11) leads to:

$$\omega_+^2 = \frac{2(\omega_{02DEG}^2 + \omega_{0g}^2)}{\kappa_1 + \kappa_3} q = \left[ \frac{4\pi e^2 n_{2DEG}}{(\kappa_1 + \kappa_3) m^*} + \frac{4e^2 v_F \sqrt{\pi n_g}}{(\kappa_1 + \kappa_3) \hbar} \right] q \quad (15)$$

Equation (15) shows that the optical plasmon frequency is proportional to root square of wave vector. Moreover, this frequency depends only on surrounding layers dielectric constant ( $\kappa_1$  and  $\kappa_3$ ). This equation also demonstrates that the dependence of optical plasmon frequency on density of

$$\omega_-^2 = q^2 \frac{\omega_{0g}^2 \omega_{02DEG}^2}{(\omega_{0g}^2 + \omega_{02DEG}^2)} \left[ \frac{2d}{\kappa_2} + \frac{(15+8\pi^2)w}{12\pi^2 \kappa_2 D} \right] = \frac{2e^2 \pi n_{2DEG} v_F \sqrt{\pi n_g}}{m^* \hbar} \left[ \frac{2d}{\kappa_2} + \frac{(15+8\pi^2)w}{12\pi^2 \kappa_2 D} \right] q^2 \quad (16)$$

Equation (16) illustrates that the solution  $\omega_-$  is proportional to wave-vector and corresponds to acoustic plasmon mode. Furthermore, the acoustic one  $\omega_- (q \rightarrow 0)$  depends on both  $\kappa_2$  (dielectric constant of contacting media) and  $\kappa_{2D}$  (dielectric constant of 2DEG sheet). Another significant point recognized from Eq.(15) and Eq.(16) is that only the analytical acoustic frequency depends on the layer-thickness of 2DEG ( $w$ ) and the distance between two layers of the system ( $d$ ) in long wavelength limit ( $q \rightarrow 0$ ).

It can be seen that the results are quite similar to those obtained by Gasser (1989) for 2DEG in double quantum well systems. The first (second) term on the second member of Eq. (15) is the square of the frequency of the optical plasmon oscillations in 2DEG (MLG) as shown by Principi *et al.* (2012) although in this paper, calculations have been done for the case of finite quantum well width. This means that for long wavelength limit, the optical frequency almost does not depend on 2DEG layer-thickness and separated distance. The main differences between results mentioned in this work and

carriers in MLG and 2DEG is significantly different (root square of  $n_{2DEG}$  and power a quarter of  $n_g$ ). This result comes from the linear dispersion at low energy range. A similar equation has been shown by Principi *et al.* (2012) although the layer-thickness has been neglected in their work.

In the case of minus sign, the second order of  $q$  must be kept because the first order reduces to zero. Calculations show:

Principi *et al.*'s (2012) ones are the form of acoustic frequency as shown in Eq. (16).

In order to make a comparison between analytical results in this paper and numerical ones from other authors, both of them are illustrated on Fig. 2 (thick lines for analytical mentioned in Eq. (11) and thin lines for numerical). The numerical results are found out by numerical solving Eq. (2) in C++ program with full form of response functions for 2DEG and MLG (Czachora *et al.*, 1982; Sarma *et al.*, 2011) and bare Coulomb interactions (Scharf and Matos-Abiague, 2012). Half-distance method is used for programming calculations, leading to two solutions as demonstrated in Fig. 2 (solid and dashed thin curves). The figure is plotted for  $\kappa_1 = \kappa_{AlGaAs} = 12.9$ ;  $\kappa_2 = \kappa_{SiO_2} = 3.9$ ;  $\kappa_3 = \kappa_{Air} = 1.0$ ;  $\kappa_{2D} = \kappa_{GaAs} = 12.9$ ; electron effective mass  $m^* = 0.067m_0$  where  $m_0$  as the vacuum mass of electron (Scharf and Matos-Abiague, 2012). Other parameters are shown in the figure. It is noted that Fermi energy and Fermi wave-vector of MLG are denoted by  $E_F$  and  $k_F$ , respectively.

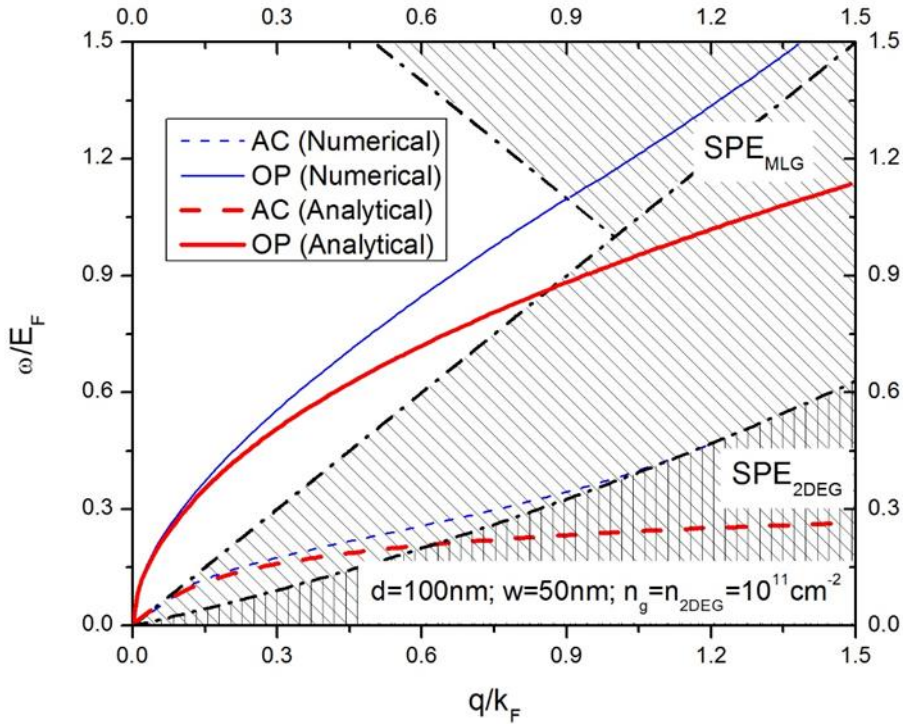


**Fig. 2: Plasmon dispersion of MLG – 2DEG system: analytical (thick lines) and numerical results (thin lines). Figure plotted for  $d = 100nm$ ,  $w = 50nm$ , and  $n_g = n_{2DEG} = 10^{11} cm^{-2}$ . Dashed-dotted lines show the boundaries of single particle excitation (SPE) region of MLG and 2DEG**

It can be seen from Fig. 2 that the analytical results obtained in Eq. (11) are almost identical to numerical ones at sufficiently small  $q$ , and present about  $q \leq 0.3k_F$  for optical branch and  $q \leq 0.5k_F$  for acoustic one. As the wave vector increases, the analytical curves go into SPE region while the numerical ones do not. The numerical optical plasmon goes nearly the MLG SPE boundary as in MLG (Hwang and Sarma, 2007), and the acoustic one touches the edges of 2DEG SPE region and disappears as plasmon of 2DEG in quantum well (Czachora *et al.*, 1982).

#### 4 CONCLUSION

In summary, the analytical plasmon oscillations frequencies of both optical and acoustic modes in MLG-2DEG double layer at zero temperature using the RPA dielectric function, taking into account the thickness of 2DEG layer and inhomogeneity of background dielectric constant have been calculated for the first time by using long wavelength expansions of response functions of 2DEG, MLG and bare Coulomb interaction. The analytical expressions show that in long wavelength limit, while the

acoustic mode is proportional to wave vector, depends considerably on spacer width, 2DEG layer-thickness, and dielectric constant of the contacting media; the frequency of optical one is proportional to root square of wave vector, almost independent on the dielectric constant and thickness of 2DEG layer. It is also proven that the density carriers in MLG and 2DEG layers have significantly different contributions in plasmon frequencies of the system.

#### ACKNOWLEDGMENT

This work is supported by An Giang University under Grant number 17.02.SP.

#### REFERENCES

- Badalyan, S. M. and Peeters, F. M., 2012. Effect of non-homogenous dielectric background on the plasmon modes in graphene double-layer structures at finite temperatures. *Physical Review* 85(19): 195444.
- Czachora, A., Holas, A., Sharma, S. R., and Singwi, K. S., 1982. Dynamical correlations in a two-dimensional electron gas: First-order perturbation theory. *Physical Review B* 25(4): 2144.

- Digish, K. P., 2015. Transport properties of monolayer and bilayer graphene. PhD thesis. The Maharaja Sayajirao University of Baroda, India.
- Gamucci, A., Spirito, D., Carrega, M., et al., 2014. Electron-hole pairing in graphene-GaAs heterostructures. *Nature Communications*, 5: 5824.
- Gasser, W., 1989. Plasmon and magneto-plasmon excitations in double heterostructures. *Zeitschrift für Physik B Condensed Matter*, 75(4): 459-468.
- Geim, A. K. and Novoselov, K. S., 2007. The rise of graphene. *Nature Materials*, 6(3): 183-191.
- Hwang, E. H. and Sarma, S. D., 2007. Dielectric function, screening, and plasmons in 2D graphene. *Physical Review B* 75: 205418.
- Hwang, E. H. and Sarma, S. D., 2009. Exotic plasmon modes of double layer graphene. *Physical Review B* 80: 205405.
- Khanh, N. Q., 1996. Dielectric function and plasmon dispersion relation. *Physica Status Solidi (b)* 197: 73.
- Khanh, N. Q., 2001. The Effect of the Image Charges on the Mobility of a Quasi-Two-Dimensional Electron Gas. *Physica Status Solidi (b)* 225(1): 89-93.
- Khanh, N. Q. and Toan, N. M., 2003. Electron correlations in two dimensions: effects of finite thickness and image charges. *Solid State Communications* 125(3-4): 133-137.
- Maier, S. A., 2007. *Plasmonics – Fundamentals and Applications*. Springer, New York.
- Men, N. V. and Khanh, N. Q., 2017. Plasmon modes in graphene-GaAs heterostructures. *Physics Letters A* 381(44): 3779-3784.
- Neto, A. H. C., Guinea, F., Peres, N. M. R., Novoselov, K. S., and Geim, A. K., 2009. The electronic properties of graphene. *Review Modern Physics* 81(1): 109.
- Principi, A., Carrega, M., Asgari, R., Pellegrini, V., and Polini, M., 2012. Plasmons and Coulomb drag in Dirac/Schrodinger hybrid electron systems. *Physical Review B* 86: 085421.
- Sarma, S. D., Hwang, E. H., and Rossi, E., 2010. Theory of carrier transport in bilayer graphene. *Physical Review B* 81: 161407.
- Sarma, S. D., Adam, S., Hwang, E. H., and Rossi, E., 2011. Electronic transport in two dimensional graphene. *Review Modern Physics* 83: 407.
- Sarma, S. D., Madhukar, A., 1981. Collective modes Spatially Separated. *Physical Review B* 23: 805.
- Scharf, B. and Matos-Abiague, A., 2012. Coulomb drag between massless and massive fermions. *Physical Review B* 86: 115425.
- Sensarma, R., Hwang, E. H., and Sarma, S. D., 2010. Dynamic screening and low energy collective modes in bilayer graphene. *Physical Review B* 82: 195428.
- Stern, F., 1967. Polarizability of a two-dimensional electron gas. *Physics Review Letters* 18(14): 546.
- Ho Sy Ta, 2017. Plasmon characteristics and dynamical properties of electrons in graphene. PhD thesis. Hanoi University of Science and Technology, Ha Noi, Vietnam (in Vietnamese).
- Tanatar, B. and Davoudi, B., 2003. Dynamic correlations in double-layer electron systems. *Physical Review B* 63: 165328.
- Tuan, D. V. and Khanh, N. Q., 2013. Plasmon modes of double-layer graphene at finite temperature. *Physica E* 54: 267-272.
- Vazifeshenas, T., Amlaki, T., Farmanbar, M., and Parhizgar, F., 2010. Temperature effect on plasmon dispersions in double-layer graphene systems. *Physics Letters A* 374(48): 4899-4903.